September 25th - 28th, 2017
INTERFACES
architecture . engineering . science IASS 2017 hamburg

Proceedings of the IASS Annual Symposium 2017
"Interfaces: architecture . engineering . science"
September 25 - 28th, 2017, Hamburg, Germany
Annette Bögle, Manfred Grohmann (eds.)

Limit state analysis of 2D statically indeterminate networks using graphic statics

Jean-François RONDEAUX*, Pierluigi D'ACUNTO[a], Joseph SCHWARTZ[a], Denis ZASTAVNI[b]

*[b]Université catholique de Louvain, Faculty of architecture, architectural engineering, urbanism (LOCI)
Place du Levant 1 (L5.05.02) – B 1348 Louvain-la-Neuve
jean-francois.rondeaux@uclouvain.be

[a] ETH Zürich, Institute of Technology in Architecture, Chair of Structural Design

Abstract

Graphic statics provides an elegant and efficient method for equilibrium analysis of various types of structures. This is particularly the case for pin-jointed frameworks, for which the use of reciprocal form and force diagrams gives direct and simultaneous insights on the static behaviour of every structural member. On the other hand, plastic theory offers a superb theoretical framework for the limit state analysis of structures presenting a certain degree of static indeterminacy as well as for equilibrium-design purposes. Based on graphic statics and plastic theory, this paper proposes a graphical methodology for the analysis of 2D statically indeterminate networks, including pin-jointed frameworks and strut-and-tie models within a continuum of material. This approach can be used for determining the collapse load factor and the corresponding collapse mechanism of existing structures, as well as for evaluating the load-bearing capacity of structures during the design process. In order to validate the methodology, the geometrically obtained collapse load factor is compared with the ones determined using classical static and kinematic approaches. The graphical methodology is then used to solve more complex cases with several degrees of static indeterminacy. Finally, the advantages for structural optimization, as well as the perspectives towards an extension to 3D networks are outlined.

Keywords: Graphic statics, plasticity theory, static indeterminacy, limit state analysis, load factor, pin-jointed frameworks, strut-and-tie models

1. Introduction

Using graphic statics for structural design is a common practice, which has been effectively evidenced by several contemporary structural engineers, such as Schwartz [18] and Baker [1]. Working on both reciprocal diagrams, optimal geometries can be determined for networks with a given connectivity of the form diagram. Authors like Beghini *et al.* [2] and Mazurek *et al.* [11] have shown that an optimization process can be applied to the set of possible solutions in order to meet specific design requirements, such as the minimization of the volume or weight of building material. Within the framework of the plastic theory, taking advantage of the lower bound theorem, solutions in equilibrium can be found that respect the boundary and yield conditions. In this respect, authors like Muttoni *et al.* [15] and more recently, Zastavni *et al.* [20] have applied graphic statics to the analysis and design of strut-and-tie models within reinforced concrete structures.

The goal of this paper is to evaluate the structural behaviour of 2D statically indeterminate networks with a given geometry and loading condition, including pin-jointed frameworks and strut-and-tie models within a continuum of material. The assumption is made here that the material shows a sufficient (nearly perfect) ductile behaviour, that no excessive deformation modifies the structural behaviour and that no instability occurs in any structural member under working loads. Buckling is avoided by limiting the compressive stresses or by confinement. In this hypothesis, we make use of the fundamental theorems of limit analysis to identify geometrically the load that brings the structure to collapse. This is done by applying an optimization process that operates on the geometric transformation of the force diagram related to the structure. The exact magnitude of this *collapse load* may be useful for theoretical purposes or in order to evaluate the risk of plastic collapse due to excessive plastic deformations.

The paper is organized in three main sections. In Section 2, we make a review of the main theoretical findings of limit state analysis used in the paper. Section 3 introduces the proposed graphical methodology for structural limit state analysis using a simple 2D network with one degree of static indeterminacy. In Section 4, we apply this methodology to the complete development of more complex 2D networks with several degrees of static indeterminacy. The last section of the paper presents a synthesis of the current results of the research and an outlook on further developments.

2. Limit state analysis and plastic theory

2.1. Collapse load factor

Given a loaded structure, the ultimate goal of limit analysis is the evaluation of the collapse load factor λ_u. This is defined as the proportionality factor that can be applied to the magnitudes of all the forces that constitute the actual loading $\{\mathbf{Q}\}$, in order to obtain the set of forces leading to the collapse of the structure $\{\mathbf{Q}\}_{\mathrm{u}}$. Equation 1 expresses this proportionality:

$$\lambda_u\{\mathbf{Q}\} = \{\mathbf{Q}\}_{\mathrm{u}} \tag{1}$$

2.2. Fundamental theorems of limit analysis

The three fundamental theorems of limit analysis may be expressed in terms of possible values for the load factor λ as follows (Heyman [8]):

- Kinematic theorem (upper bound theorem): any load factor λ_k calculated from a kinematically compatible mechanism is greater than or equal to the collapse load factor λ_u.
- Static theorem (lower bound theorem): any load factor λ_s calculated from a statically compatible distribution of internal forces and applied loads that respect the yield conditions is lower than or equal to the collapse load factor λ_u.
- Uniqueness theorem: the collapse load factor is unique.

Inequations 2 express synthetically these three theorems:

$$\lambda_{k,i} \geq \lambda_u \geq \lambda_{s,j} \tag{2}$$

where $\lambda_{k,i}$ is the load factor corresponding to the i^{th} kinematically compatible mechanism of collapse and $\lambda_{s,j}$ the load factor corresponding to the j^{th} statically compatible distribution of forces.

2.3. Kinematic and static approaches

Based on the fundamental theorems of limit analysis, approaches for limit state analysis of structures may be classified in two categories: kinematic ones and static ones.

The kinematic approaches aim at finding the exact – therefore, minimum – value for λ_k by identifying the collapse mechanism and determining its related load factor. Since the plastic behaviour of the material at collapse implies that the superposition principle of structural actions cannot be applied, all the possible kinematically compatible mechanisms and their corresponding load factors $\lambda_{k,i}$ should be taken into account in order to obtain the actual collapse load factor $\lambda_u \stackrel{def}{=} \min_i \lambda_{k,i}$. It is common to use energetic considerations on rigid-body-like mechanisms (Marti [10]). The principle of virtual works (PVW) benefits from the fact that the work originated from the external forces and the one resulting from the internal stresses are equal (Thompson and Haywood [19]). Adapted to pin-jointed frameworks, this can be written as:

$$\sum_P (\mathbf{q}_P \cdot \boldsymbol{\delta}_P) = \sum_b (\mathbf{f}_b \cdot \boldsymbol{\Delta}\mathbf{L}_b) \tag{3}$$

with $\mathbf{q}_P$ the external load vector applied to node P, $\boldsymbol{\delta}_P$ the displacement vector of node P, $\mathbf{f}_b$ the internal normal force acting on bar b, and $\boldsymbol{\Delta}\mathbf{L}_b$ the extension of bar b.

This method is very efficient when it comes to finding the value of the load factor $\lambda_{k,i}$ associated with every kinematically compatible mechanism i. Yet, the potential high amount of possible mechanisms and their kinematical complexity remain clear drawbacks. Furthermore, the given solutions for these load factors are *unsafe* in the sense that Inequation 2 states that they all are upper bound values for the actual collapse load factor λ_u. This means that being able to know only an incomplete subset of all the possible mechanisms may lead to overestimating the bearing capacity of the structure.

Static approaches have been developed taking into account the successive plasticisation of elements when increasing the load factor until the structure is turned into a mechanism. Every possible load factor $\lambda_{s,j}$ obtained using a static approach that respects the boundary and yield conditions should be calculated, so that $\lambda_u \overset{def}{=} \max\limits_j \lambda_{s,j}$ (Rjanitsyn [16]). A classical method consists in studying the internal forces distribution by means of superimposition of free and reactant diagrams in equilibrium on statically determinate sub-structures. As already observed, the final force distribution must satisfy the equilibrium and yield conditions. If this distribution is such that the full plastic resistance is reached in a sufficient amount of bars as to form a mechanism, then value of the load factor obtained is the collapse one. Contrary to the kinematic, this approach can be regarded as *safe*. Indeed, were some of the statically admissible distributions of forces to be omitted, this incomplete analysis would only lead to an underestimation of the effective collapse load factor λ_u.

3. Limit state analysis and reciprocal diagrams

3.1. Self-stress states and mechanisms in reciprocal diagrams

Using graphic statics for limit state analysis of 2D networks implies to manipulate their form and force diagrams. They constitute dual structures that provide graphical insight into each other, especially when assessing mechanisms and states of self-stress (Mitchell *et al.* [14] and McRobie *et al.* [12]). Each state of self-stress that can be identified in the form diagram corresponds to a static indeterminacy. For networks with an underlying planar graph, this assessment can be done considering the Maxwell rigidity number N for 2D as modified by Calladine [4]:

$$N = 2v - b - 3 = m - s \tag{4}$$

where m is the number of mechanisms and s the number of independent self-stress states. The rigidity number N of one of the dual structures and the one N^* of its reciprocal are related by (Micheletti [13]):

$$N + N^* = -2 \tag{5}$$

For a given 2D network without internal mechanisms, its degree of static indeterminacy can be identified. Every degree of static indeterminacy of the form diagram corresponds to a degree of freedom in the complete force diagram. This degree of freedom consists in a particular transformation of the force diagram that is equivalent to an *offset* (Mitchell *et al.* [14] and McRobie *et al.* [12]). In this transformation of the force diagram, all the forces keep their direction unchanged. Only those forces that are involved in the transformation change their magnitudes.

In Figure 1, a simple 2D network is taken into account. Since the given structure has an underlying planar graph and no mechanisms, according to Equation 4: $N = m - s = 0 - 2 = -2$. Therefore, the

Maxwell rigidity number N^* of the reciprocal force diagram $\mathbf{F}^*$ should be equal to zero in order to respect Equation 5. From the initial structure two independent states of self-stress can be created by removing the nodes 3 and 5 respectively, each of them being characterized by reciprocal form and force diagrams (respectively $\mathbf{F_1}$-$\mathbf{F_1}^*$ and $\mathbf{F_2}$-$\mathbf{F_2}^*$). Each self-stressed force diagram can be traced at an independent scale. When assembling these two states of self-stress the resulting form diagram **F** is two times statically indeterminate and the force diagram $\mathbf{F}^*$ has two degrees of freedom that are related to two independent offsets. Considering the force diagram $\mathbf{F}^*$ as a dual structure of **F**, this presents one state of self-stress and one mechanism, so that $N^* = 1 - 1 = 0$ as expected by Equation 5. In case one of the states of self-stress is fixed, the force diagram $\mathbf{F}^*$ has only one degree of freedom left and can be transformed by moving one of its nodes without changing the directions of its edges. Thanks to this transformation, all the possible configurations of $\mathbf{F}^*$ can be explored. The graphical methodology introduced in the next section takes advantage of this property.

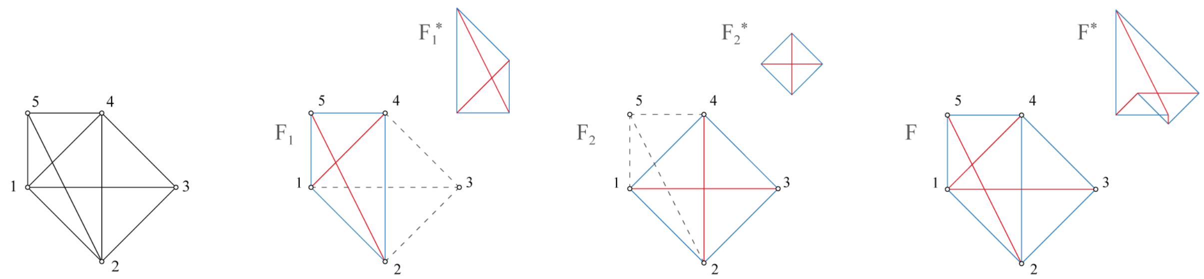

Figure 1: Two independent self-stress states ($\mathbf{F_1}$, $\mathbf{F_2}$) are obtained from a given 2D network with two degrees of static indeterminacy. Their reciprocal force diagrams ($\mathbf{F_1}^*$, $\mathbf{F_2}^*$) are drawn, each with a different chosen scale. Assembling the diagrams gives a complete form **F** and force $\mathbf{F}^*$ diagrams of the given network.

3.2. A graphical methodology to evaluate the limit load

The graphical methodology that we propose can be organized into a sequence of six steps:

1. We first identify the degree of static indeterminacy of the given form diagram **F**. This gives the amount of independent statically determinate form diagrams $\mathbf{F_i}$ that can be constructed upon **F** through independent self-stress states, including the one produced by the external loads ($\mathbf{F_{ei}}$).

2. For each $\mathbf{F_i}$ defined in the previous step, we trace the corresponding force diagram $\mathbf{F_i}^*$ following the Bow's notation (Bow [3]). Each diagram is drawn using an arbitrary scale factor s_i. As the limit load factor λ_u is a proportionality factor, a specific scale factor s_{ei} can be fixed at will for the external forces $\mathbf{q_i}^*$ and the resulting $\mathbf{F_{ei}}^*$.

3. The independent force diagrams $\mathbf{F_i}^*$ are then assembled into one single force diagram $\mathbf{F}^*$ related to the initial statically indeterminate form diagram **F**. To assemble the diagrams, a vectorial addition of the corresponding vectors in $\mathbf{F_i}^*$ is performed. Considering the external loads fixed, each $\mathbf{F_i}^*$ corresponds to a degree of freedom of $\mathbf{F}^*$ since they can all be drawn at a random scale, independently from the scale s_{ei} chosen for the diagram of the external loads $\mathbf{F_{ei}}^*$.

4. Given $\mathbf{F}^*$ and considering the external loads fixed, we detect each degree of freedom of the diagram, which correspond to an offset of $\mathbf{F}^*$. As previously explained, in these transformations the direction of the force vectors in $\mathbf{F}^*$ is invariant, so that the $\mathbf{f_{ij}}^*$ and $\mathbf{q_i}^*$ stay parallel to themselves. Each geometric transformation is then parametrized and $\mathbf{F}^*$ is consequently regarded as a parametric force diagram $\mathbf{F_p}^*$. For each degree of freedom of $\mathbf{F_p}^*$ a parameter x_n is defined as the position of a node P_n of $\mathbf{F_p}^*$ along the line of action of one of the forces $\mathbf{f_{ij}}^*$ connected to P_n; based on P_n, the position of all the other nodes of $\mathbf{F_p}^*$ are defined through geometrical constructions. As such, the variation of all the x_n describes the overall geometric transformation of $\mathbf{F_p}^*$.

5. We then apply an optimization process to the variation of the x_n defined in the previous step in order to minimize the highest of the absolute magnitudes $|\mathbf{f}_{ij}^*|$ of the force vectors $\mathbf{f}_{ij}^*$ in the parametric force diagram $\mathbf{F}_p^*$. In this process, the magnitudes $|\mathbf{q}_i^*|$ of the external loads $\mathbf{q}_i^*$ are kept constant. Since the $|\mathbf{q}_i^*|$ are proportional to the $|\mathbf{f}_{ij}^*|$, minimizing $|\mathbf{f}_{ij}^*|$ is equivalent to maximizing the load factor λ_s. Out of this step, the collapse force diagram $\mathbf{F}_u^*$ is found.

6. The exact value of the collapse load factor λ_u can eventually be found by scaling the entire collapse force diagram $\mathbf{F}_u^*$ so that the highest magnitude $|\mathbf{f}_{ij}^*|$ is exactly equal to the given maximum allowable ultimate normal force $|\mathbf{f}_u^*|$.

3.3. Validation of the method

In order to validate the graphical methodology described in the previous section, we apply it to the 2D network of Figure 1, this time regarding one of the self-stress states as generated by external loads. The result is compared to the ones obtained using conventional approaches of limit analysis: complete static limit analysis (graphical and analytical) and complete kinematic limit analysis (Rondeaux *et al.* [17]).

Following the graphical methodology described in Section 3.2, we first define the form ($\mathbf{F}_{e1}$, $\mathbf{F}_2$) and force ($\mathbf{F}_{e1}^*$, $\mathbf{F}_2^*$) diagrams of the self-stressed states of the given network. Here, the diagrams $\mathbf{F}_{e1}$ and $\mathbf{F}_{e1}^*$ are related to the self-stress state generated by the three external forces. The diagrams are drawn using arbitrary scale factors within the digital CAD environment *McNeel Rhinoceros*. Then, we assemble $\mathbf{F}_{e1}^*$ and $\mathbf{F}_2^*$ and, using the parametric tool *Grasshopper*, we construct a parametric force diagram $\mathbf{F}_p^*$ where the external loads are fixed. Here we define the position of node P^* along the line of action of $\mathbf{f}_{24}^*$ of $\mathbf{F}_p^*$ as the parameter of the optimization process. In this process, we minimize the highest of the absolute magnitudes $|\mathbf{f}_{ij}^*|$ of the force vectors in $\mathbf{F}_p^*$. The collapse form $\mathbf{F}_u$ and force $\mathbf{F}_u^*$ diagrams are obtained, with the identification of the collapse load $\mathbf{q}_u^*$ and of the plasticized bars $\mathbf{f}_{12}$ and $\mathbf{f}_{14}$ for which $|\mathbf{f}_{12}^*| = |\mathbf{f}_{14}^*| = |\mathbf{f}_u^*|$. The solution found gives a ratio $|\mathbf{q}_u^*|/|\mathbf{f}_u^*| = \lambda_s = 0.707$. The optimization functions that are dealt with in the proposed graphical methodology are in general non-linear. A global optimization algorithm such as an evolutionary algorithm, can be used in the first place in order to locate an intermediate solution close to the global optimum. Afterwards, provided that the function is continuous, the optimization problem can be solved using a gradient-based algorithm. The algorithms used to solve the optimization problems treated in this section and in the followings are the ones included in the *Grasshopper* plugin *Goat* (Flöry *et al.* [7]), which relies on the *NLopt* library (Johnson [9]).

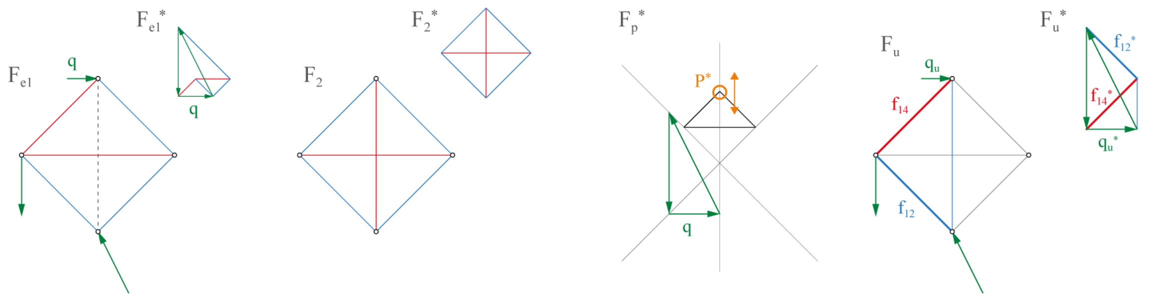

Figure 2: Application of the proposed graphical methodology for the limit analysis of a network with one degree of static indeterminacy: form ($\mathbf{F}_{e1}$, $\mathbf{F}_2$) and force ($\mathbf{F}_{e1}^*$, $\mathbf{F}_2^*$) diagrams of the self-stressed states; parametric force diagram ($\mathbf{F}_p^*$); collapse form diagrams ($\mathbf{F}_u$) with identification of the plasticized bars $\mathbf{f}_{12}$ and $\mathbf{f}_{14}$; collapse force diagram ($\mathbf{F}_u^*$) with identification of the magnitude of the collapse load $\mathbf{q}_u^*$ and $|\mathbf{f}_{12}^*| = |\mathbf{f}_{14}^*| = |\mathbf{f}_u^*|$.

As a first test to validate the proposed methodology, considering the simplicity of this case study, it is possible to apply here a complete static limit analysis and obtain graphically all the limit configurations. Each of them corresponds to a limit force diagram $\mathbf{F}_u^*$ and is obtained by setting the value $|\mathbf{f}_u^*|$ for two of the six internal forces $\mathbf{f}_{ij}^*$ (i, j = 1 to 4). The fifteen possible combinations result in the eight geometrically different limit force diagrams ($\mathbf{F}_{u1}^*$ to $\mathbf{F}_{u8}^*$) shown in Figure 3, where the imposed value $|\mathbf{f}_u^*|$ is represented with thick lines. Four limit force diagrams ($\mathbf{F}_{u5}^*$ to $\mathbf{F}_{u8}^*$) do not respect the yield condition since the magnitude of some of the internal forces $|\mathbf{f}_{ij}^*|$ is higher than $|\mathbf{f}_u^*|$; according to the static theorem, these may not be considered as possible forces distributions. When comparing the magnitudes $|\mathbf{q}_i^*|$ of the external loads for each of the four remaining limit force diagrams ($\mathbf{F}_{u1}^*$ to $\mathbf{F}_{u4}^*$), using the theorems of plasticity we can detect the force diagram corresponding to collapse. This one is the diagram where the external loads have the highest magnitude. In this very simple case, this limit force diagram can be immediately identified as $\mathbf{F}_{u1}^*$. Moreover, we can deduce geometrically the static load factor $|\mathbf{q}_u^*|/|\mathbf{f}_u^*| = \lambda_s = \sqrt{2}/2 = 0.707$. The values of the load factor for the various limit cases studied using this complete static limit analysis (graphical) are presented in Table 1.

In addition, a static limit analysis of the pin-jointed structure of Figure 2 is done manually using a traditional analytical method such as in Rjanitsyn [16]. A self–stress state, generated by imposing the magnitude of the normal force in one of the overabundant bars, is superposed to the state of stress produced by the external forces on a statically determinate structure. The magnitude obtained for the load factor is once again $Q_u / N_u = \sqrt{2}/2 = 0.707$ where Q_u is the magnitude of the load applied on node 4 and N_u the ultimate normal force of the bars. For networks with a more complex geometry, this type of analysis can be performed on the equivalent pin-jointed framework through traditional FEM software.

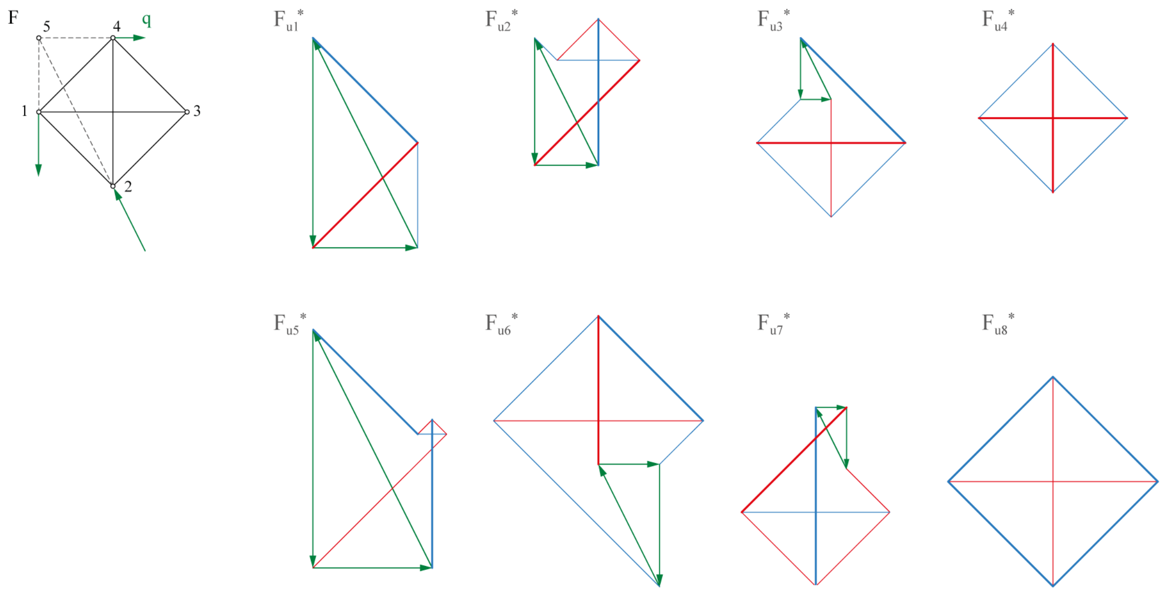

Figure 3: Eight limit force diagrams are obtained by transforming the initial force diagram $\mathbf{F}^*$ of Figure 1. In each diagram, the magnitude of two forces $\mathbf{f}_{ij}^*$ (thick lines) is set to $|\mathbf{f}_u^*|$. Limit force diagrams $\mathbf{F}_{u5}^*$, $\mathbf{F}_{u6}^*$, $\mathbf{F}_{u7}^*$, $\mathbf{F}_{u8}^*$ do not respect the yield condition since the intensity of at least one of their forces is bigger than $|\mathbf{f}_u^*|$. $\mathbf{F}_{u1}^*$ is the collapse force diagram because the external loads reach here their highest magnitude.

Regarding the structure as a pin-jointed framework, we then use a complete kinematic limit analysis (Figure 4) based on the principle of virtual works (PVW) to find the collapse mechanism and the corresponding collapse load factor λ_u. Applying a complete kinematic analysis to the equivalent pin-jointed framework leads to the same conclusion as before, since the collapse load factor: $\lambda_u = Q_u / N_u = \min_i \lambda_{k,i} = \sqrt{2}/2 = 0.707$. Because this value is exactly the same as the one obtained for the limit force diagram $\mathbf{F_{u1}}$* where $|\mathbf{f_{14}}^*|=|\mathbf{f_{12}}^*|=\mathbf{f_u}^*$, Equation 2 is verified and the proposed graphical methodology is validated. The kinematic load factors for all the kinematically compatible mechanisms are listed in Table 1 and the lowest value amongst them is identified for the collapse mechanism $M_{14/12}$, where bars 14 and 12 are plasticized.

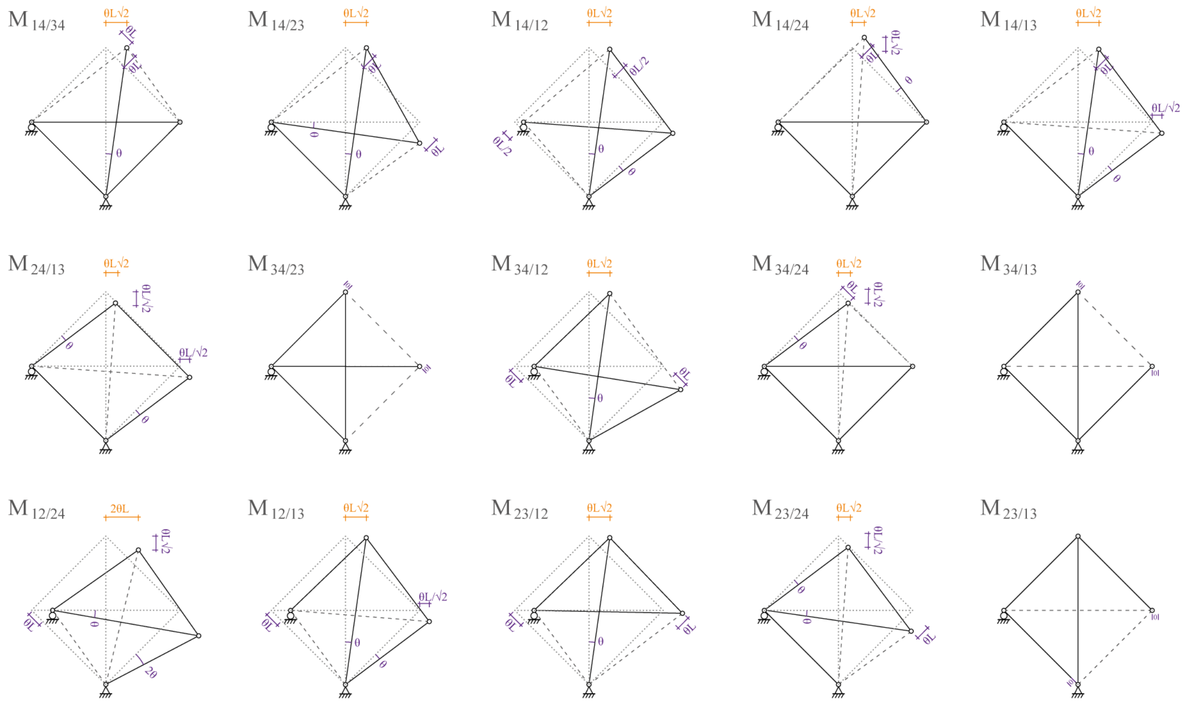

Figure 4: Kinematically compatible mechanisms for the pin-jointed framework equivalent to case of Figure 2.

Kin. comp. mechanism	**Kinematic load factor:** Q_u/N_u		**Limit force diagram**	**Static load factor:** $\lvert\mathbf{q_u^*}\rvert/\lvert\mathbf{f_u^*}\rvert$
$M_{14/34}$	$\sqrt{2}$		$\mathbf{F_{u8}}^*$	Yield not respected
$M_{14/23}$	$\sqrt{2}$		$\mathbf{F_{u8}}^*$	Yield not respected
$\mathbf{M_{14/12}}$	$\mathbf{\sqrt{2}/2}$		$\mathbf{F_{u1}}^*$	$\mathbf{\sqrt{2}/2}$
$M_{14/24}$	$1+\sqrt{2}/2$		$\mathbf{F_{u2}}^*$	$\sqrt{2}-1$
$M_{14/13}$	$1+\sqrt{2}/2$		$\mathbf{F_{u7}}^*$	Yield not respected
$M_{34/23}$	No Mechanism		$\mathbf{F_{u8}}^*$	Yield not respected
$M_{34/12}$	$\sqrt{2}$		$\mathbf{F_{u8}}^*$	Yield not respected
$M_{34/24}$	$1+\sqrt{2}/2$		$\mathbf{F_{u6}}^*$	Yield not respected
$M_{34/13}$	No Mechanism		/	Impossible equilibrium
$M_{23/12}$	$\sqrt{2}$		$\mathbf{F_{u8}}^*$	Yield not respected
$M_{23/24}$	$1/2+\sqrt{2}/2$		$\mathbf{F_{u6}}^*$	Yield not respected
$M_{23/13}$	No Mechanism		/	Impossible equilibrium
$M_{12/24}$	$1/2+\sqrt{2}/2$		$\mathbf{F_{u5}}^*$	Yield not respected
$M_{12/13}$	$1+\sqrt{2}/2$		$\mathbf{F_{u3}}^*$	$\sqrt{2}/2-1/2$
$M_{24/13}$	1		$\mathbf{F_{u4}}^*$	0

Table 1: The kinematic load factors relative to the 15 kinematically compatible mechanisms (Fig. 4) are compared to the static load factors obtained by geometrical relations in the possible limit force diagrams (Fig. 3). The collapse mechanism, collapse force diagram and their corresponding load factor are marked in bold.

4. Case studies

In order to test the proposed graphical methodology, we apply it to the complete development of two 2D networks with more than one degree of static indeterminacy. Following the sequence described in Section 3.2, for each case study we first detect the degrees of static indeterminacy and build form and force diagrams for every state of self-stress of the structure. We then assemble a parametric force diagram and eventually run the optimization process to evaluate the collapse load factor.

In the first case study shown in Figure 5, a structure with two degrees of static indeterminacy is taken into consideration. The parametric force diagram $\mathbf{F_p}^*$ is optimized with respect to the positions of the nodes P_1^* and P_2^*. The collapse force diagram $\mathbf{F_u}^*$ is obtained and the resulting collapse load factor can be compared to the one calculated by applying a kinematic limit analysis on the corresponding collapse mechanism; both approaches give the same result: $\lambda_s = \lambda_k = \lambda_u = 1.762$.

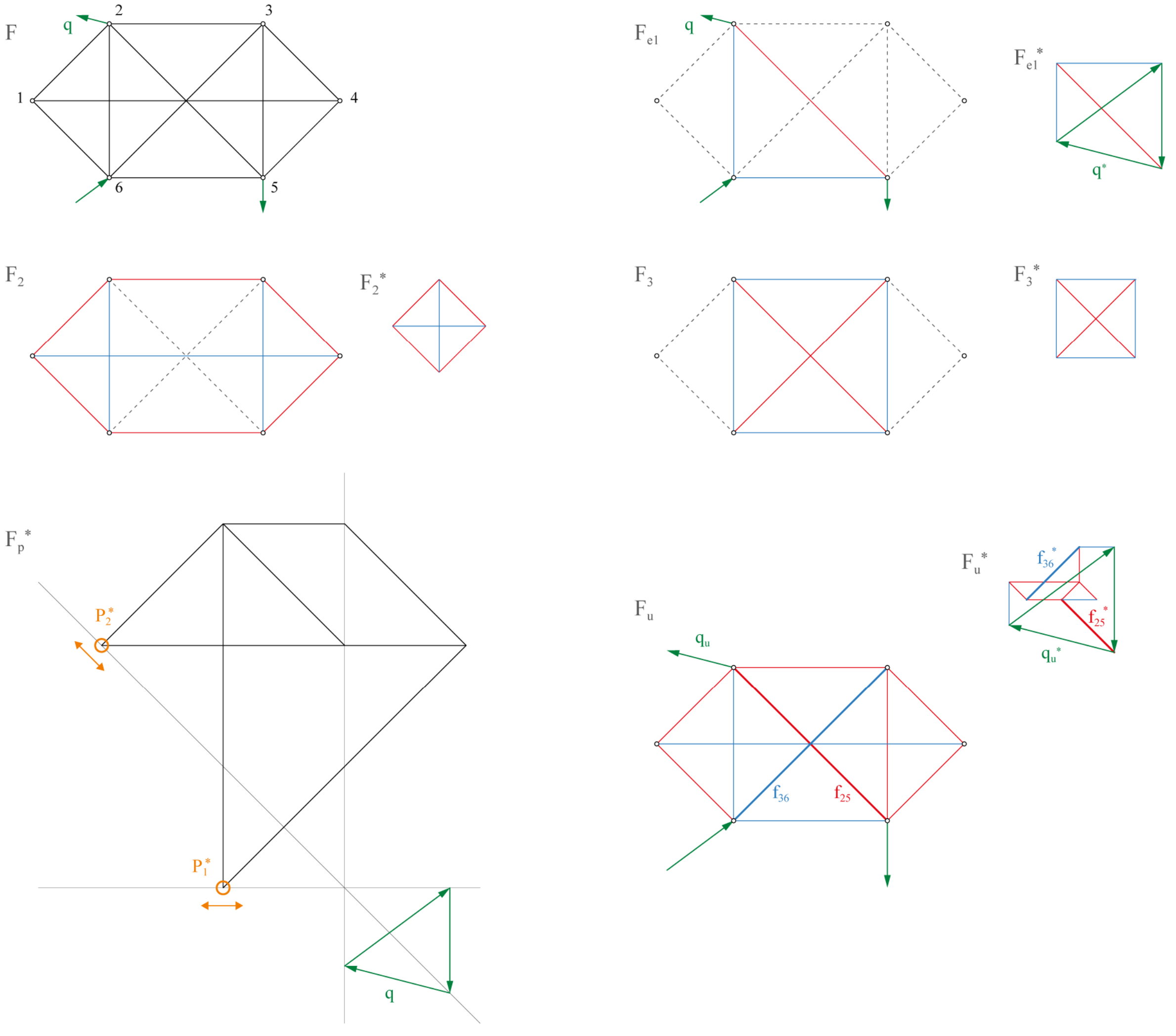

Figure 5: Application of the proposed graphical methodology to a network with two degrees of static indeterminacy.

In the second example illustrated in Figure 6, the same optimization procedure is applied on the positions of three nodes (P_1^*, P_2^*, P_3^*) of $\mathbf{F_p}^*$ to find $\mathbf{F_u}^*$. Once again, the collapse load factor obtained with the proposed graphical methodology is equal to the kinematic one calculated with a kinematic limit analysis: $\lambda_s = \lambda_k = \lambda_u = 1.155$.

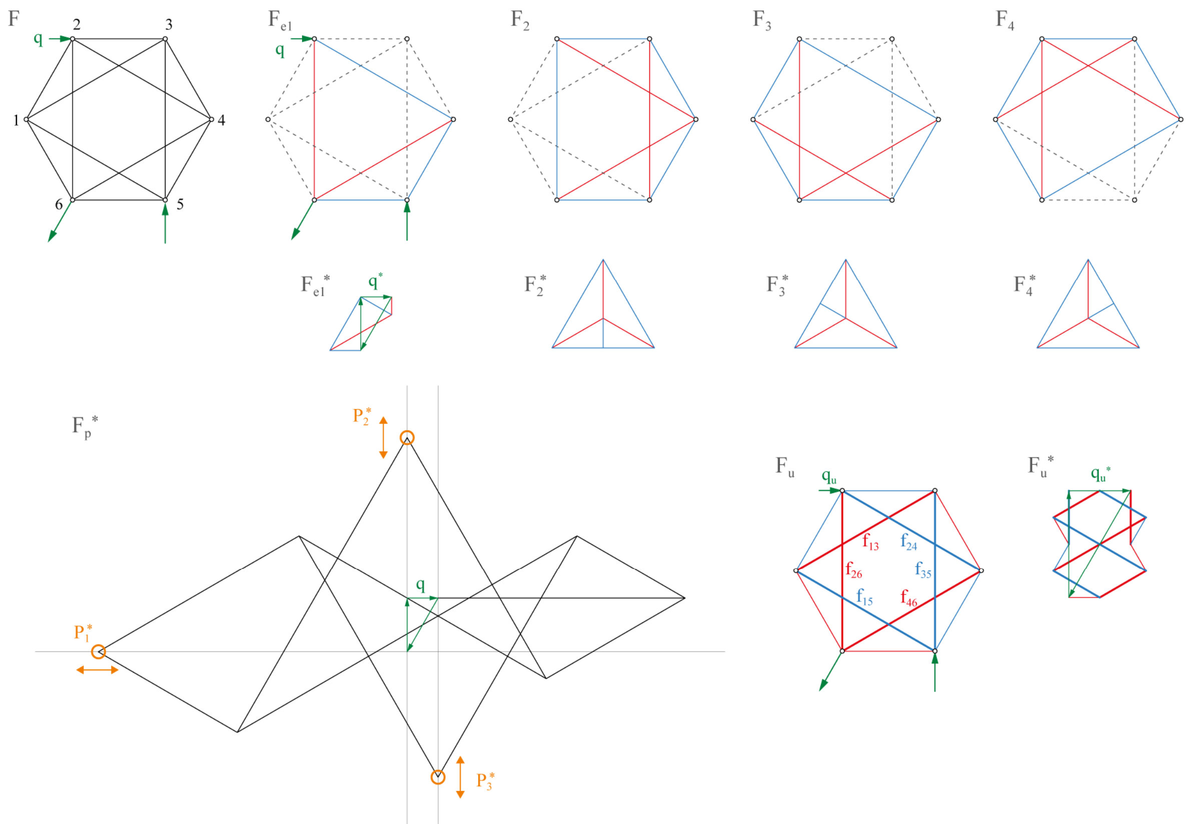

Figure 6: Application of the proposed graphical methodology to a network with three degrees of static indeterminacy.

5. Conclusions and future work

This paper has extended the scope of application of graphic statics to the limit analysis of 2D statically indeterminate networks. When associated with optimisation procedures, graphic statics proves to be an efficient tool for this field of structural analysis. The proposed graphical methodology is implemented within a parametric digital software and takes advantage of the properties of reciprocal form and force diagrams. It is supposed that perfect plastic redistribution is possible and that no local instability can occur so that the lower bound theorem of plasticity remains valid. Each degree of freedom of the force diagram is described by the position of one of its nodes along a given direction. These positions constitute a set of variables related to the self-stress states of the form diagram that can be manipulated using optimization techniques. Compared to other available methods for limit state analysis, the proposed graphical methodology converts the analytical static problem of finding the collapse load factor into a problem of geometric optimization. Thanks to this, the exploration of the design space can be immediately visualized, while the use of form and force diagrams gives direct and simultaneous insights on the static behaviour of the structure.

Further development of the research will take into account the different behaviours of tensile and compressive edges of a given network; the question of buckling will be specifically addressed. Moreover, future work will aim at the extension of the proposed graphical methodology to the third dimension. In this regards, the transformation of the 3D force diagram of statically indeterminate spatial networks (D'Acunto *et al.* [5]), will be used for the optimization process.

References

[1] Baker W. F., Beghini L.L, Mazurek A., Carrion J. and Beghini A., Maxwell's Reciprocal Diagrams and Discrete Michell Frames. *Structural Multidisciplinary Optimization*, 2013; **48**: 267–277.

[2] Beghini L. L., Carrion J., Beghini A., Mazurek A., Baker. W. F., Structural optimization using graphic statics. *Structural Multidisciplinary Optimization*, 2014; **49**: 351–366.

[3] Bow R., Economics of Construction in Relation to Framed Structures. London, 1873.

[4] Calladine C. R., Buckminster Fuller's *Tensegrity* Structures and Clerk Maxwell's Rules for the Construction of Stiff Frames. *International Journal of Solids and Structures.* 1978; **14**: 161–172.

[5] D'Acunto P., Jasienski J.P., Ohlbrock P.O., Fivet C., Vector-Based 3D Graphic Statics: Transformations of Force Diagrams, in *Proceedings of the IASS 2017*, Abstract accepted.

[6] Fivet C. and Zastavni D., A fully geometric approach for interactive constraint-based structural equilibrium design. *Computer-Aided Design*, 2015; **61**; 42-57.

[7] Flöry S., Schmiedhofer H., Reis M., Goat, http://www.rechenraum.com/en/goat/overview.html (accessed 04/2017).

[8] Heyman J., *Basic structural theory*. Cambridge University Press, 2008.

[9] Johnson S., The NLopt optimization package, http://ab-initio.mit.edu/nlopt (accessed 04/2017).

[10] Marti P., *Theory of Structures.* Wiley-VCH Verlag GmbH & Co. KGaA, 2013.

[11] Mazurek A., Beghini A., Carrion J. and Baker W., Minimum weight layouts of spanning structures obtained using graphic statics, *International Journal of Space Structures*, 2016; **31** (2-4); 112 – 120.

[12] McRobie A., Baker W., Mitchell T. and Konstantatou M., Mechanisms and states of self-stress of planar trusses using graphic statics, part II, *Int. Journal of Space Structures*, 2016; **31** (2-4); 102-111.

[13] Micheletti A., On generalized reciprocal diagrams for self-stressed frameworks. *International Journal of Space Structures*, 2008; **23(3)**; 153-166.

[14] Mitchell T., Baker W., McRobie A. and Mazurek A., Mechanisms and states of self-stress of planar trusses using graphic statics, part I, *Int. Journal of Space Structures*, 2016; **31** (2-4); 85 –101.

[15] Muttoni A., Schwartz J. and Thürlimann B., *Design of concrete structures with stress fields*. Birkhäuser, 1996.

[16] Rjanitsyn A.R., *Calcul à la rupture et plasticité des constructions.* Eyrolles, 1959.

[17] Rondeaux J.-F. and Zastavni D., Graphical limit state analysis of hyperstatic structures, in *Proceedings of the IASS Annual Symposium 2016.* Tokyo, 2016.

[18] Schwartz J., The Art of Structure, in *Proceedings of the International Conference on Structures and Architecture ICSA.* Guimaraes, 2016

[19] Thompson F. and Haywood G.G, *Structural Analysis using Virtual Work.* Chapman and Hall Ltd, 1986.

[20] Zastavni D., Deschuyteneer A., and Fivet C., Admissible geometrical domains and graphic statics to evaluate constitutive elements of structural robustness. *International Journal of Space Structures*, 2016; **31(2-4)**:165-176.